Video Article

Electronic Measurements of Cellular Adhesion Using Field-Effect Transistor Cell-Substrate Impedance Sensing (FETCIS)

Jessica Ka-Yan Law[1], Anna Susloparova*[1], Dieter Koppenhöfer*[1], Xuan Thang Vu[1], Felix Hempel[1], Sven Ingebrandt[1]

[1]Department of Informatics and Microsystem Technology, University of Applied Sciences Kaiserslautern

*These authors contributed equally

Correspondence to: Sven Ingebrandt at sven.ingebrandt@fh-kl.de

URL: http://www.jove.com/video/52430
DOI: doi:10.3791/52430

Keywords: Field-Effect Transistor Cell-substrate Impedance Sensing (FETCIS), label-free, real-time, cell adhesion, cancer cell, confluent culture, single cell, pharmacology

Date Published: 11/21/2014

Citation: Law, J.K.Y., Susloparova, A., Koppenhöfer, D., Vu, X.T., Hempel, F., Ingebrandt, S. Electronic Measurements of Cellular Adhesion Using Field-Effect Transistor Cell-Substrate Impedance Sensing (FETCIS). *J. Vis. Exp.* (), e52430, doi:10.3791/52430 (2014).

Abstract

In this work, Field-Effect Transistor Cell-substrate Impedance Sensing (FETCIS) is proposed to examine cellular adhesion on protein-coated transistors with improved spatial resolution. Cellular adhesion is often used as an indicator in many in vitro cytotoxicity assays. However, most of those assays involve staining dyes which may interfere with the tested compounds. In our approach, FETCIS is used to detect impedance changes of the transistors due to cellular adhesion and detachment processes. Compared to the commercially available Electrical Cell-substrate Impedance Sensing (ECIS) systems, the size of the detection transistors of FETCIS can reach down to a single cell and even subcellular resolution. In the present study, FET devices with flat topography were designed and fabricated to enhance better cellular attachment and to shift the recorded effects to a lower frequency range. To verify the sensitivity of FETCIS, confluent, low density, and single cell cultures were tested with the system. Chemical and mechanical removal of confluent cultures and single cell from the transistor were performed and clear impedance changes due to the absence and presence of cells were observed. With the help of a simplified, equivalent electrical circuit model, the measured impedance spectra can be explained. Furthermore, the FETCIS system was used for real-time monitoring of the effects of anti-cancer drug and nanoparticles on cancer cells. The results of our study indicate the applicability of FETCIS for cancer research and for analyzing pharmacological effects of the tested compounds opening up new possibilities in future ECIS assays.

Introduction

Field-effect devices have been used for several biomedical applications ranging from the detection of cancer marker proteins[1] and DNA[2] to cells[3]. The main advantage of such devices is their high sensitivity to changes in surface potential at the liquid-solid interface. For cell-adhesion studies, a device with comparable size of a single cell is preferable and silicon-based field-effect transistors (FET) fit into these needs. Compared to the commercially available Electrical Cell-substrate Impedance Sensing (ECIS) system which based on gold electrodes[4,5], the FETs are not limited to the size of the sensors and thus can be applied to study single cells. Typical sizes of the commercial metal electrodes in ECIS range from 25 µm to 250 µm in diameter. Due to the limited size of the detection electrodes, collective instead of individual responses of cells are measured. The data obtained from such averaged cell populations might conceal individual reactions associated to the heterogeneous properties of cells[6]. Therefore it should be of interest for certain specific applications to analyze individual reactions of cells. In the present study, an impedance system using FET, named Field-Effect Transistor Cell-substrate Impedance Sensing (FETCIS), for detecting cell adhesion is presented.

Electronic transistor-transfer function (TTF) was measured in the present study. A combination of bandwidth limiting effect of reference electrode, electrolyte solution, the cell covering the transistor, the transistor itself including contact lines on chip, and the first amplifier stage, are reflected by the measured TTF spectrum. By applying a sinusoidal signal with 10 mV amplitude and varying frequency from 1 Hz to 1 MHz via the reference electrode, changes in bandwidth caused by attaching different biological samples to the gate oxide of the FETs were identified[3,7]. Responses of the biological sample to the AC voltage are frequency-dependent. From the recorded frequency spectrum of the system, characteristics and properties of the attached biological sample can be deduced[8]. Generally an electronic transfer function, denoted as H in the present study, is defined by the ratio of the input and the output voltage of the amplifier. It is the signal transfer of a sinusoidal signal between the reference electrode input U_{in} and the signal output after the transimpedance amplifier stage U_{out} **(Figure 1)**. With our in-house built FETCIS system, only the real part of the TTF is recorded[9]. This system was further optimized and with the help of a fast lock-in amplifier full spectra including amplitude and phase information can be recorded, which were used to interpret the recorded effects[9].

To fully explain the recorded spectra, the FET device in contact with an adherent cell can be described using an equivalent-electrical circuit (EEC) **(Figure 1)**, which is derived from the most simple point-contact model[10]. This model was described before and is typically applied as the easiest approach to explain extracellular recorded action potentials from neurons[11,12] or cardiac myocytes[13]. In brief, the capacitance of the adherent cell membrane C_M, the resistance of the cell membrane R_M, and the resistance of the thin, electrolyte-filled cleft between the cell and transistor R_{seal} represent the passive element of the EEC model. The cellular membrane is further divided into free (C_{FM}, R_{FM}) and attached parts (C_{JM}, R_{JM}). The contact line capacitances and resistances of source and drain are included in the EEC with C_{source}, C_{drain} and R_{source}, R_{drain}, respectively. A combined resistance R_{el} is represented by the reference electrode and the electrolyte. In order to optimize the FETCIS sensor

for highest resolution in TTF recordings, different simulations have been performed[14]. Sensitive FETCIS sensors show large TTF differences between the cell-adhered and the cell-free case and in addition these effects are favorable to be observed at lower frequencies due to cheaper instrumentations. Based on the simulation results, a new generation of FET device was designed and fabricated for this project.

In order to understand the TTF spectra, an analytical equation representing the transfer function of the EEC has been derived[15]. In this equation several parameters need to be considered, which result in the typical shape of the measured TTF spectra. These parameters include chip-related parameters, transimpedance circuit parameters, and cell-related parameters. By fitting the measured TTF spectrum to the equation, cell-related parameters (R_{seal} and C_M) can be obtained, which indicate the status of the cell. The R_{seal} value indicates how tight the cell adheres on top of the transistor, while the C_M value indicates the shape of the cell. These two cell parameters change according to the cell attachment and detachment processes. The influences of the R_{seal} and C_M on the TTF spectra have been studied by simulation of the EEC circuit in PSpice, a program for electrical circuit simulation. In **Figure 2** an idealized cell detachment process from the transistor surface is shown where the cell does not change its shape during detachment and is only lifted up, stepwise. The figure shows the simulated TTF spectra varying R_{seal} in a range of 1 MΩ to 400 kΩ. By increasing R_{seal}**(Figure 2, from model 5 to model 1)**, a gradual increase of the signal amplitude between 20 and 200 kHz is observed, while the complete removal of the cell can be clearly distinguished from the cell-attached case **(Figure 2)**. On the other hand, the value of the C_M changes when the morphology of the cells is changing during detachment or as a response to external stimuli. In **Figure 3**, an adherent cell is gradually deformed during the detachment process. Simulation was performed by modelling an adherent cell as a hemisphere and a gradually detaching cell from the transistor surface with different spherical caps but keeping the total surface area of the cell membrane constant. In this model, the C_M value is correlated to the ratio changes of the attached to free membrane area. The simulated TTF spectra show that decreasing C_M values lead to smaller TTF amplitude **(Figure 3, from model 1 to model 5)**. With the above simulation results, the TTF spectra changes due to cell attachment and detachment can now be better understood. For a complete picture, however, recordings on a fixed frequency are not enough. For time-dependent processes, recordings of the full spectra and fitting to the model should be done in order to extract the time evolution of the cell-related parameters from the model[15,16], like it was earlier described for ECIS.

In the following manuscript, new FET devices according to previous simulations were designed and fabricated. In order to show that our FETCIS system is feasible and sensitive enough to measure the cellular attachment and detachment processes, different cell types were cultured on the FET devices and their respective TTF spectra were measured. As mentioned earlier, the detection sensitivity of the FET devices is not limited by the size of the transistors. Therefore, it is possible to study the adhesion of single cell using the present FETCIS system. Furthermore, our FETCIS system has been successfully demonstrated as an electronic platform to monitor real-time drug effects on cell adhesions.

Protocol

1. Preparation of the FET devices and cell cultures

1. Fabrication and encapsulation of the quasi-planar FETs
    1. Clean the 4 inch n-type silicon wafer using a modified protocol based on standard Radio Corporation of America (RCA) protocol[17].
    2. Wet thermally grow silicon oxide (SiO_2) on the silicon wafer in the Centrotherm oven at 1000 °C for 5 hours.
        1. Load wafers to a quartz wafer holder and load wafer holder to the loader of the oven. Flow N_2 (3 SLM) through the quartz tube of the oven. Heat the tube to 800 °C, check temperature homogeneity in the tube (± 5 °C)
        2. Load wafers to the center of the tube. Increase temperature to 1000 °C, check temperature homogeneity in the tube (± 5 °C). Heat up the water in the bubbler to 90 °C.
        3. Turn off N_2 flow, turn on O_2 flow (0.5 SLM) through bubbler. The output of the bubbler was connected to the input of the quartz tube. Start count down time to 0.
        4. Turn off O_2 flow and disconnect the output of bubbler to the output of the quartz tube. Connect the N_2 (3 SLM) flow through the tube. Turn off the heating power of the quartz tube and let it evolve.
        5. When the temperature of the oven reaches 800 °C, unload wafer out of the oven. Wait for 2 hours (wafer temperature is equal to room temperature). Remove wafers from the wafer holder and put to the storage box.
        NOTE: All the valves and connection in the oven were controlled automatically by an oven controller software.
    3. Define the contact lines using optical lithography with a positive photoresist (AR-P3100) (Supplementary note: Mask 1). Expose the wafer with aligned optical mask to UV light. Expose the resist on the contact lines to UV light and develop using a developer (AR 300-26: H_2O_2 =1:1 (v/v)) [17].
    4. Etch SiO_2 of the exposed areas by dipping in buffered hydrofluoric acid (BHF) for 16 min.
    5. Remove the photoresist by acetone and isopropanol and then clean the wafer by RCA cleaning protocol[17].
    6. Implant boron ions on the wafer with a dose of $1 \cdot 10^{16}$ ions/cm^2 and energy of 150 keV using commercial services.
    7. Clean the wafer in piranha solution for 10 min at 60 °C and then dip in 1% hydrofluoric acid (HF) for 30 seconds.
    8. Anneal the wafer in in 100% N_2 atmosphere at 1000 °C for 1 h in the Centrotherm oven.
    9. Define the source and drain electrode areas using a second optical lithography (positive resist AR-P3100) and etch SiO_2 on the exposed areas (same parameters as steps 1.1.3, 1.1.4) (Supplementary note: Mask 2).
    10. Remove the photoresist by acetone and isopropanol and then clean the wafer by RCA cleaning protocol[17].
    11. Implant boron ions on the wafer with a dose of $1 \cdot 10^{15}$ ions/cm^2 and an energy of 80 keV using commercial services.
    12. Etch all SiO_2 layers on the wafer in BHF solution for 15 min as in step 1.1.4. Clean the wafer by the RCA protocol[17].
    13. Anneal the wafer for 5 min in 100% N_2 at 950 °C and then wet oxidation for 60 min at 950 °C. See detail in 1.1.2. Temperature in step 1.1.2.5 was set to 950 °C.
    14. Define the gate area and the electrical contacts of source and drain by a third optical lithography using positive photoresist (AR-P3100) (Supplementary note: Mask 3). See detail in 1.1.3.
    15. Wet-etch the wafer by dipping in BHF solution for 3 min and then in 1% HF until the SiO_2 is totally etched. Remove the resist by acetone and isopropanol.
    16. Clean the wafer by the RCA protocol[17]. Afterwards, thermally grow a 6 nm thick SiO_2 as gate dielectrics using a dry oxidation protocol.
        1. Heat the oven up to 800 °C, flow N_2 (3 SLM) through the tube.

2. Load wafer into the tube. Heat the oven up to 820 °C. Turn off N_2 flow, flow O_2 (0.5 SLM) through the oven and wait for 45 min.
3. Turn off O_2 flow, turn on N_2 flow. Turn the heating off.
4. Wait the temperature of the oven reaches 800 °C, unload wafer from the tube. Wait for 2 hours (wafer temperature is equal to room temperature). Remove wafers from the wafer holder and put to the storage box.

17. Spin coat AR U4040 on wafer (2000 rpm, 60 s) and heat the wafer at 90 °C for 2 min. Expose the resist-coated wafer with source and drain contacts mask (Supplementary note: Mask 4) under a broadband UV for 6 s (36 mJ/cm^2) and then post-bake at 115 °C for 5 min.
    1. Completely expose the wafer without mask under a broadband UV for 20 s (120 mJ/cm^2). Finally develop the resist in developer (AR-300-46: H_2O_2 = 1:3 (v/v) for 20 s and then rinse in DI water.
18. Wet-etch the SiO_2 on the source and drain contacts by submerging in 1% HF for 2 min directly before the metal evaporation.
19. Deposit a metal stack of 200 nm of aluminum (rate 5 A/s, power 48%), then 20 nm of titanium (rate 5 A/s, power 25%) and lastly 100 nm of gold (rate 5 A/s, power 21.5%) using electron beam evaporation.
20. Lift-off the metal on the resist on the wafer in acetone for 20 min with the help of an ultrasound source. Clean wafer by isopropanol and dry wafer with N_2 gas.
21. Anneal the wafer at 400 °C in 100% N_2 for 10 min.
22. Protect the wafer by a resist and cut the 4 inch wafer to obtain the individual 7×7 mm^2 FET chips.
23. Sonicate the FETs in acetone for 5 min to remove the protection resist. Repeat the sonication step with new acetone and then isopropanol.
24. Apply a small amount of epoxy 377 to the middle of a 68-pin Leaded Chip Carrier. Glue the FET at the center and bake the FET device for 1 h at 150 °C.
25. Wire bond the FET to the carrier using aluminum wire. Use wedge-wedge bond techniques for the wire bonding[18].
26. Mix the silicon adhesive 96-083 in the ratio of 1:10. Apply a thin layer of the silicon adhesive mixture to two glass rings with inner diameters of 3 mm and 17 mm, respectively.
27. Glue the small glass ring to the center of the FET and the big glass ring on the carrier to form a cell culture chamber using the silicon adhesive 96-083 mixture. Bake the FET device for 30 min at 120 °C.
28. Fill in the space between the small and big glass rings with silicon adhesive 96-083 mixture. Bake the FET device for 1 h at 130 °C.

2. Cleaning and coating of the FET device for cell cultures
    1. Clean the FET surface with 70% ethanol soaked cotton buds. Sonicate the FET devices in distilled water (5 min), 2% Hellmanex III solution (5 min), and then distilled water (5 min).
    2. Dry the FET device and put 20 µl of 20% sulfuric acid to the FET surface. Incubate the FET device for 30 min at 80 °C. Sonicate the FET device in distilled water for 5 min.
    3. Fill the FET chamber with 1 ml of 70% ethanol and wait for 5 min. Replace the 70% ethanol with sterile distilled water. Repeat for 3 times.
    4. Dry the FET devices under the laminar flow.
    5. Add 10 µl of 0.1 mg/ml fibronectin to the FET surface and incubate for 3 h at 37 °C. Afterwards, remove the fibronectin and rinse the FET device with sterile distilled water once.
    6. Add 50 µl of cell suspension (confluent culture: 10,000 to 20,000 cells; low density culture: 1,000 to 3,000 cells) to each FET device and wait for 30 min. Then add 1 ml of respective culture medium to fill up the FET chamber. Incubate for 24 h under standard condition (37 °C, 5% CO_2) before impedance measurement.
        1. For human malign melanoma SkMel28 cells, use Dulbecco's Modified Eagle's Medium (supplemented with 10% Fetal Calf Serum, 10,000 U/10 mg Penicillin/Streptomycin and 20 mM L-Glutamine in 100 ml of the medium).
        2. For human Embryonic Kidney HEK293 cells, use Minimal Essential Medium (supplemented with 10% Fetal Calf Serum, 10,000 U/10 mg Penicillin/Streptomycin, 20 mM L-Glutamine, 1% Non-Essential Amino Acid, and 50 mg G418 in 100 ml of the medium).
        3. For human lung adenocarcinoma epithelial H441 cells, use Roswell Park Memorial Institute medium (supplemented with 10% Fetal Calf Serum, 10,000 U/10 mg Penicillin/Streptomycin and 20 mM L-Glutamine in 100 ml of the medium).

2. Impedimetric analysis of cellular adhesion and detachment

1. Connect the portable 16-channel amplifier system to the measurement computer. Connect the FET device with cultured cells to the amplifier. Insert an external Ag/AgCl reference electrode to the cell chamber of the FET and connect to the amplifier.
2. Start the BioMol software. Measure the drain-source current of all 16 FET devices by applying gate-source voltage (50 measurement points, from 0 V to -3 V) at constant drain-source voltage (0 V, -1 V, -2 V, -3 V).
3. As the program calculates the transconductance value (g_m) automatically by dividing the measured drain-source current with the applied gate-source voltage, set drain-source and gate-source voltages to the values at which transconductance is maximum.
4. Apply 10 mV signal ranging from 1 Hz and 1 MHz via the Ag/AgCl reference electrode. Measure TTF from 16 transistors simultaneously within 1 min.
5. Switch off the amplifier. Disconnect the reference electrode and the FET device from the amplifier system. Replace the medium in the cell chamber of the FET with 0.5% trypsin. Incubate the FET device for 30 min at 37 °C.
6. Switch on the amplifier. Reconnect the FET device and reference electrode to the amplifier. Set the voltages to the same value as in 2.3. Measure the impedance of the transistor again as step 2.4.

3. Verification of the single cell impedance measurement

1. Measure the TTF from the FET devices with low density cell culture.

2. Pull a patch-clamp pipette with diameter of 10-15 µm (Parameters for the pipette puller: Heat = 400, Filament = 5, Velocity = 20, Delay = 200, Pull = 0).
3. Place the patch-clamp pipette next to a single adhered cell on the transistor. Suck the patch-clamp pipette in order to apply under pressure for the single cell to attach on the patch-clamp pipette. Remove the cell by moving away the patch-clamp pipette under the Differential Interface Contrast microscope.
4. Measure the TTF in the range of 1 Hz and 1 MHz again as step 2.4.

4. Real-time monitoring of the effect of nanoparticles and topotecan hydrochloride on human lung cells

1. Prepare the FET devices as described in step 1.2.
2. Dilute NexSil20 nanoparticles to a concentration of 60 µg/ml and 600 µg/ml; and topotecan hydrochloride to a concentration of 10 µg/ml, in H441 culture medium[8,9].
3. Characterize the FET device with cultured cells as described in step 2.1 to 2.4.
4. Place the portable amplifier system into a regulated incubator (37 °C, 5% CO_2). Replace the culture medium with NexSil20- or topotecan hydrochloride-containing medium. Start the time-dependent TTF measurement at a constant 200 kHz frequency and measure for 2 h and 30 min.
5. Measure the TTF in the range of 1 Hz and 1 MHz again as step 2.4.

Representative Results

Quasi-planar FET devices have been fabricated and used in the present study (**Figure 4**). Each FETCIS has 16 individual transistors (25 µm in width and 5 µm in length) with a distance of 200 µm in between. The FET devices have an almost flat SiO_2 surface **(Figure 5a)** with only a 220 nm step height at the 16 transistors gates **(Figure 5b)**. Flat topography is important for migration and cellular adhesion experiments. Previously, cells preferentially adhered to the edges of the contact lines instead of the sensor area **(Figure 6a)**. With the optimized flat topography, cells are widely spread on the whole device surface **(Figure 6b)**.

Confluent and low density cell cultures were used in the present study in order to prove that the sensitivity of the FET devices and the amplifier system can reach down to single cell resolution. Human malign melanoma cells with polygonal morphology were used as an example in this case. The FET surface is completely or partially covered by the cells **(Figure 7a and Figure 7b)**. Using FETCIS, significant differences in the spectra were observed between the cell-free and cell-covered transistors in both confluent and single cell cultures **(Figure 7c and Figure 7d)**. The results show that our FET devices and amplifier system are suitable for detecting cell adhesion from confluent down to single cell cultures. To further confirm the single cell measurements, TTF of a transistor with an adhered single cell was measured before and after this cell was mechanically removed by a patch-clamp pipette. A clear difference was observed between the spectra **(Figure 8)**.

In order to use the present system as a pharmacological platform to study cytotoxicity drug effects on cancer cells, the standard anti-cancer drug topotecan hydrochloride and silica nanoparticles NexSil20 were applied to the H441 human lung cancer cells cultured on the FET devices. Real-time cell detachment processes due to drug cytotoxicity were monitored by FETCIS. Compared to the transistors without cells on top (Channel 14), significant changes in the spectra (Channel 9, 10, 13) were observed after the administration of the drug **(Figure 9)**. To extend the application of our electronic platform to study other possible anti-cancer drugs, NexSil20 nanoparticles were tested against the lung cancer cells. The nanoparticles led to an increase of signal amplitude after 30 min **(Figure 10)** indicating cellular apoptosis or necrosis.

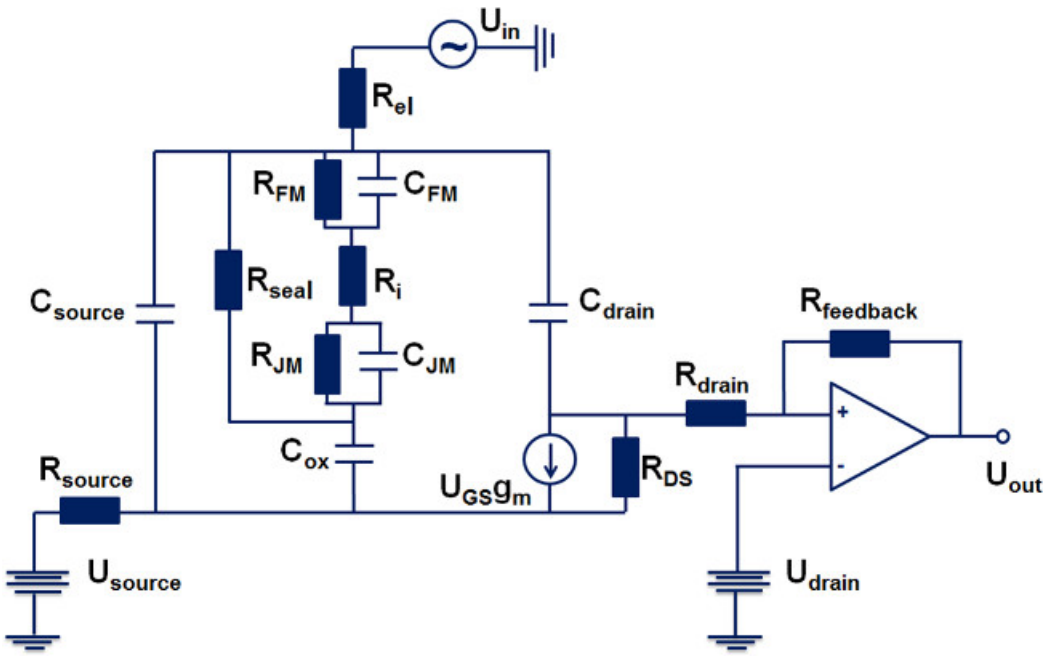

Figure 1: An equivalent electronic circuit, which describes an FET device in contact with an adherent cell on top of the transistor gate. The cell membrane is typically divided into a free part (C_{FM}, R_{FM}) and a part in the cellular junction (C_{JM}, R_{JM}). To complete this circuit, the inner resistance of the cell (R_{in}) and the electrolyte-filled cleft of the junction area (R_{seal}) are included. Chip-related elements include gate oxide capacitance (C_{ox}), the transconductance (g_m), and the output resistance (R_{DS}). The parasitic parameters like contact line capacitances and series resistances of source and drain are contributing to the EEC with C_{source}, C_{drain} and R_{source}, R_{drain}, respectively. The reference electrode and the electrolyte solution contribute as a combined series resistance R_{el}. This figure has been modified from[14].

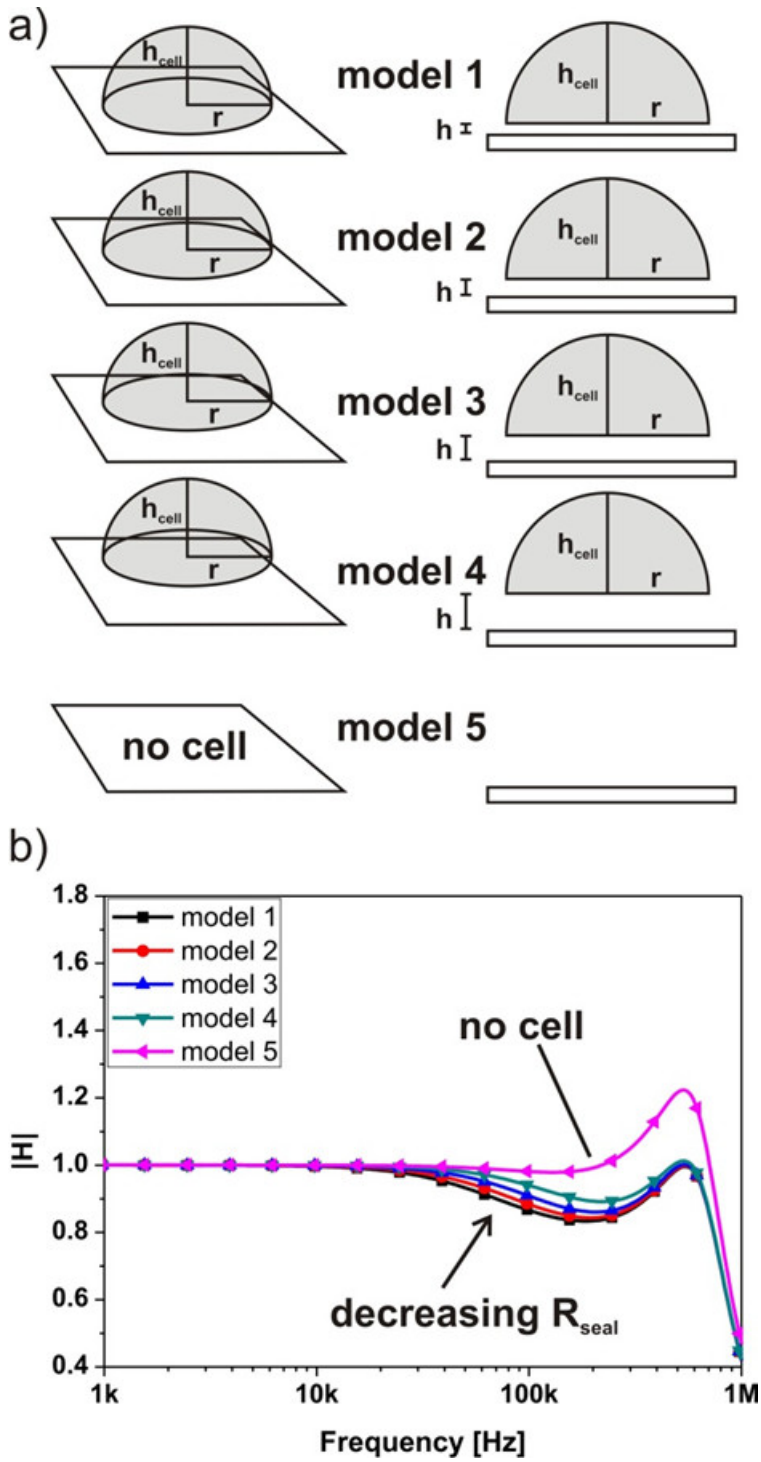

Figure 2: Modelling of the cellular detachment from the transistor surface without changes in cell morphology. The detaching cell from model 1 to model 5 does not change its shape during the detachment process. TTF spectra changes by varying the distance between the cell and the transistor (seal resistance R_{seal}) in a wide range (from 1 MΩ to 400 kΩ).

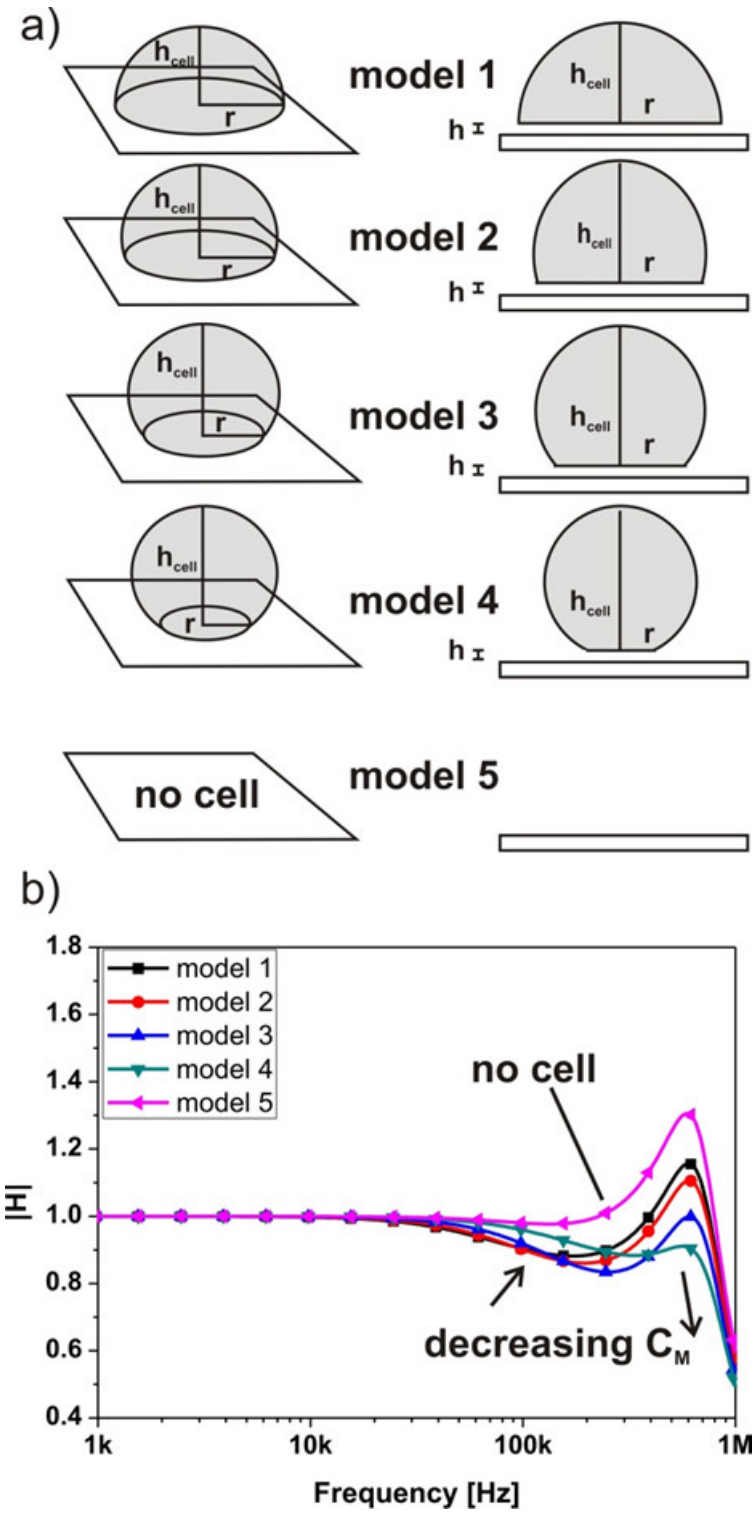

Figure 3: Modelling of an adherent cell to the transistor surface with simple geometrical shape changes. During detachment, there is a reduction in cell attached area and an increase in cell height. The simulated TTF spectra for cell-covered transistor gate (model 1), transistor gate with the gradually detached cell (model 2 - 4) and for cell-free transistor gate (model 5) are shown.

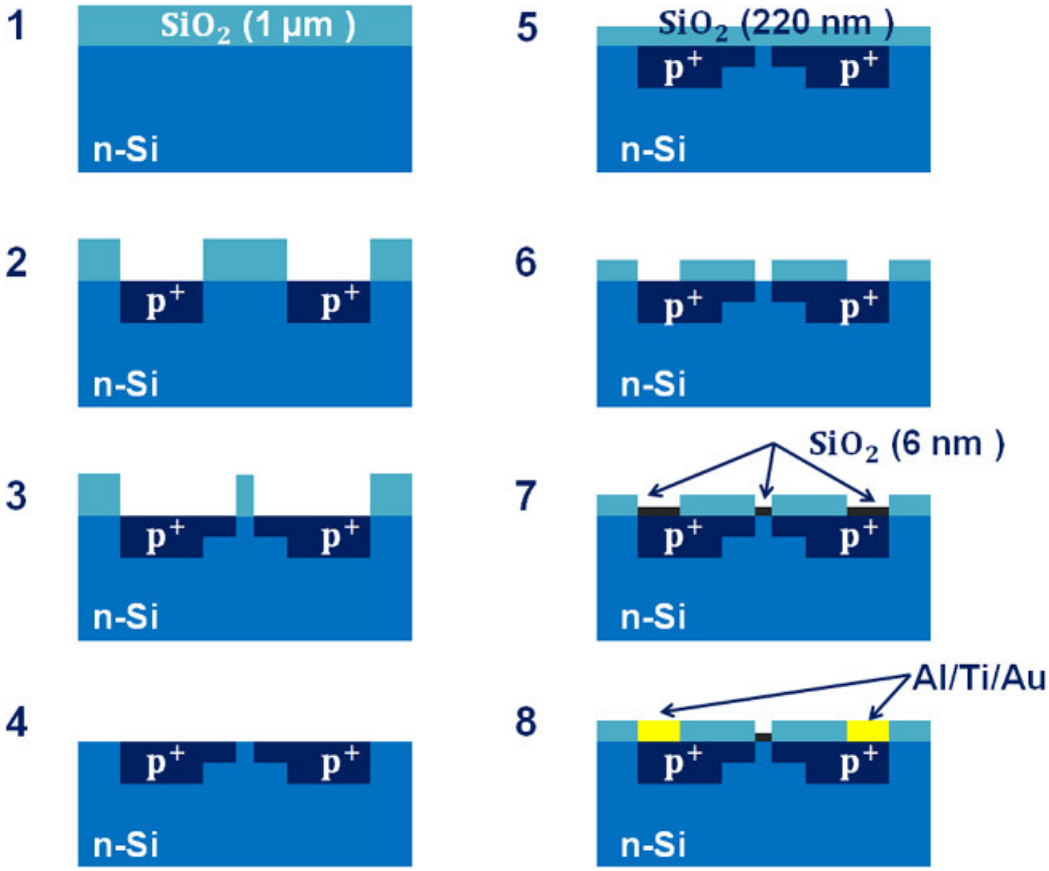

Figure 4: Schematic cross-section of the FET device fabrication process. (1) Wet oxidation to grow 1 µm thick of SiO_2 on the n-type silicon wafer. (2) Defining the source and drain contact lines: first optical lithography, wet-etching of SiO_2 in HF, boron ions implantation, and dopen activation. (3) Defining the source and drain of the FET: second optical lithography, shallow boron ions implantation. (4) Complete removal of all SiO_2 layer on the wafer. (5) Growth of 220 nm of SiO_2 as passivation layer. (6) Open the FET's gate and the source and drain contacts against the oxide passivation layer: third optical lithography, wet-etching of SiO_2. (7) Dry oxidation to grow 6 nm SiO_2 as gate insulator. (8) Metallization of the source and drain contacts using lift-off techniques: fourth optical lithography, etching of SiO_2 on the contacts, Al/Ti/Au metal deposition, lift-off in acetone, ohmic contact formation by annealing at 400 °C in N_2 atmosphere. This figure has been modified from[14].

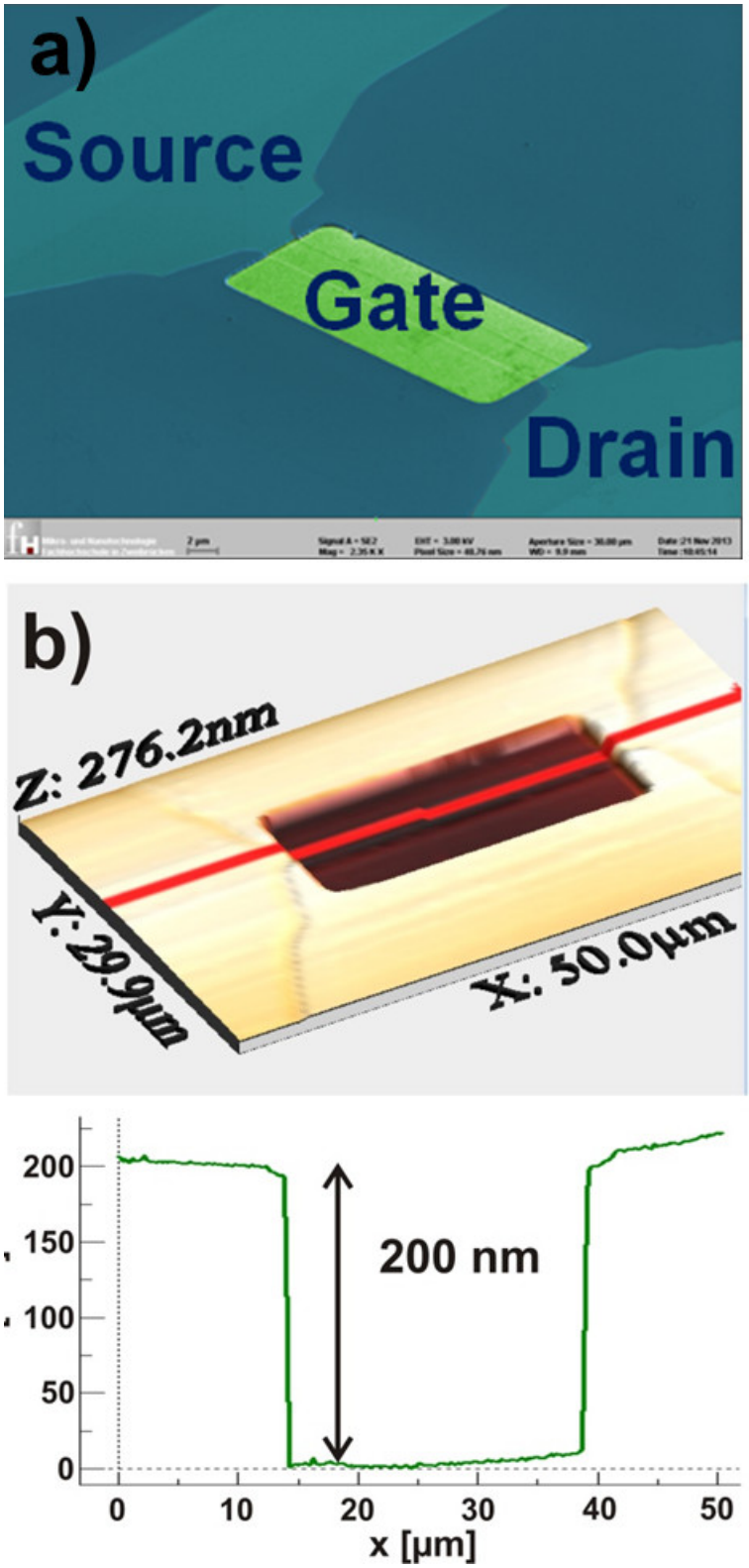

Figure 5: Close-up and AFM images of the planar field-effect transistor surfaces. Zoom in to an individual gate contact opening with the gate dimensions 5×12 µm^2 (Scanning electron microscopy, colored) (a). The modification of the fabrication protocol resulted in a much flatter chip surface, where only the gate areas are embedded in about 220 nm deep holes (b). This figure has been modified from[14].

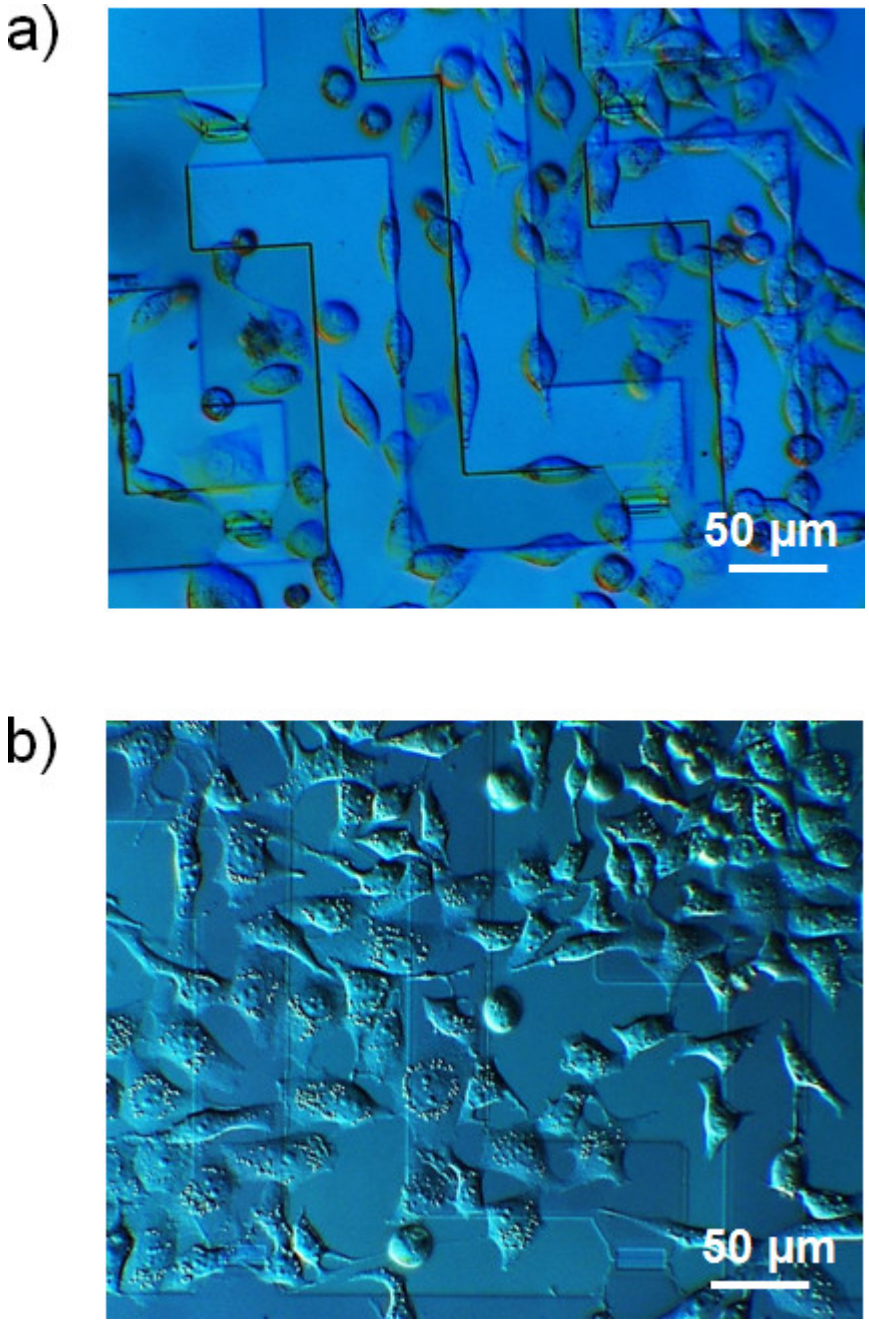

Figure 6: Microscopic images of the HEK293 cells on the former and the new FET devices. Preferential adhesion of cells to the edges of the contact lines on the surfaces can be observed on the former device (a). Flatter cell morphologies can be observed on the new designed device (b). This figure has been modified from[14].

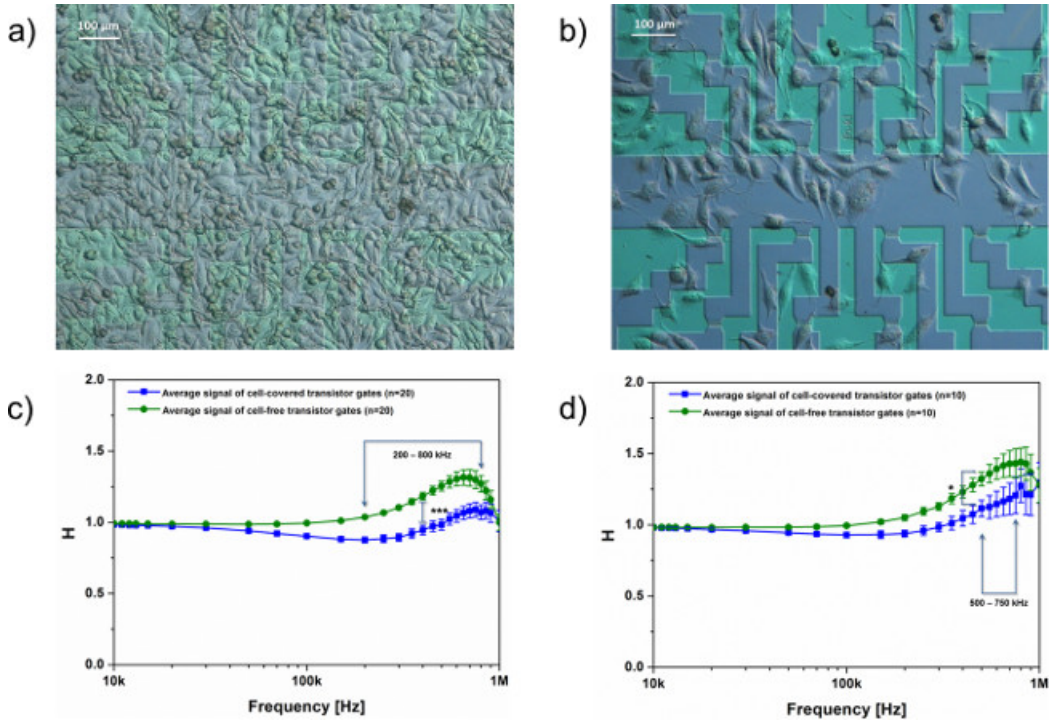

Figure 7: Microscopic images and transistor-transfer functions (TTF) of the transistor gates covered by confluent and low density of SkMel28 cells. SkMel28 cells have a polygonal morphology and are cultured on fibronectin-coated transistor surfaces. Confluent cell culture (a) and adhered single cells (b) on individual transistors can be achieved by optimizing the number of cells seeded on the FET surfaces. By measuring the TTF, significant differences between the cell-covered and cell-free transistors were measured in a frequency range of 200 to 800 kHz ($p < 0.001$, $n = 20$) (c). Similar result was obtained in low density culture, where significant differences were observed in a frequency range of 500 to 750 kHz ($p < 0.05$, $n = 10$) (d). Please click here to view a larger version of this figure.

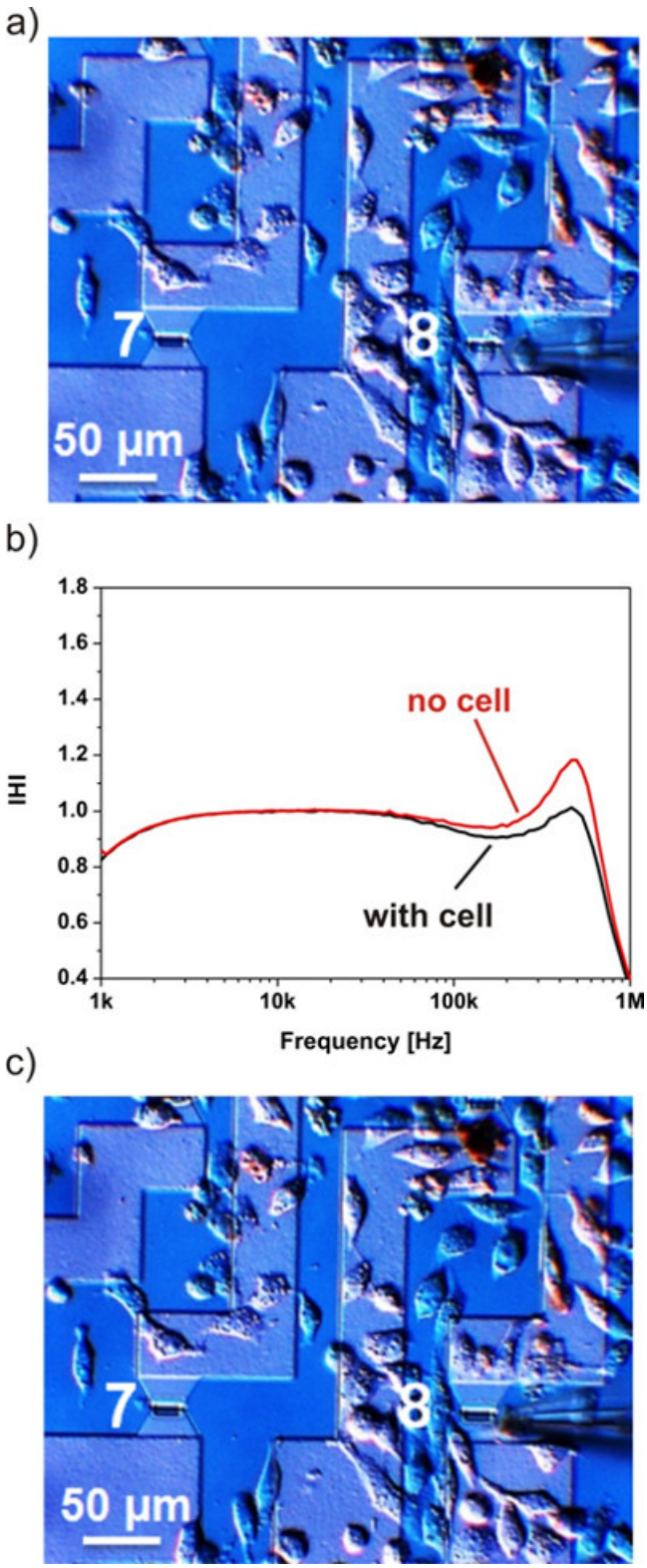

Figure 8: Microscopic images and transistor-transfer functions (TTF) of the transistor gates before and after the removal of a single adhered cell with a patch-clamp pipette. Microscopic image of two transistor gates is shown (a). Transistor gate 8 is covered by a single HEK293 cell while transistor gate 7 is cell-free. Comparison of the TTF spectra for the transistor gate 8 before and after removal of the single cell with a patch-clamp pipette (b). Microscopic image after removal of the HEK293 cell from the transistor gate 8 with a patch-clamp pipette is shown (c).

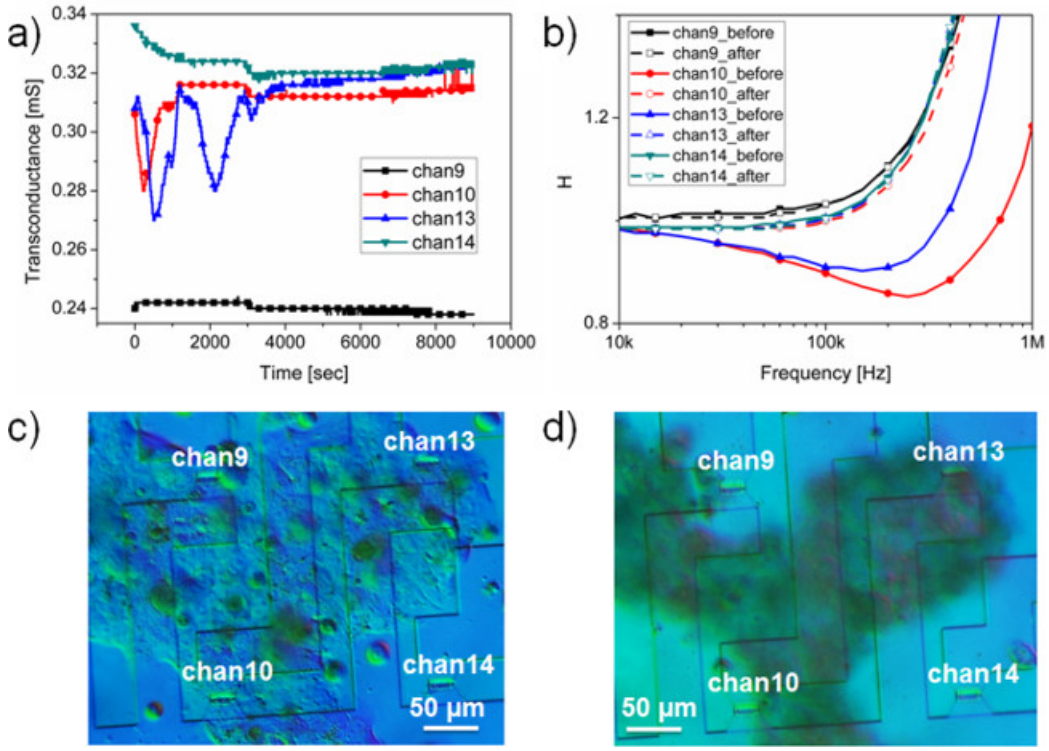

Figure 9: Time-dependent measurement of the anti-cancer drug effects on H441 cells. Real-time measurements at a constant frequency of 200 kHz of the transistors are shown (a). Changes in signal amplitudes are observed within 1 h. Recorded impedance spectra before and after the administration of topotecan hydrochloride (b). Microscopic image of H441 on the FET device is shown (c). Morphological changes of the cells due to the application of topotecan hydrochloride after 2 h and 30 min (d). This figure has been modified from[9]. Please click here to view a larger version of this figure.

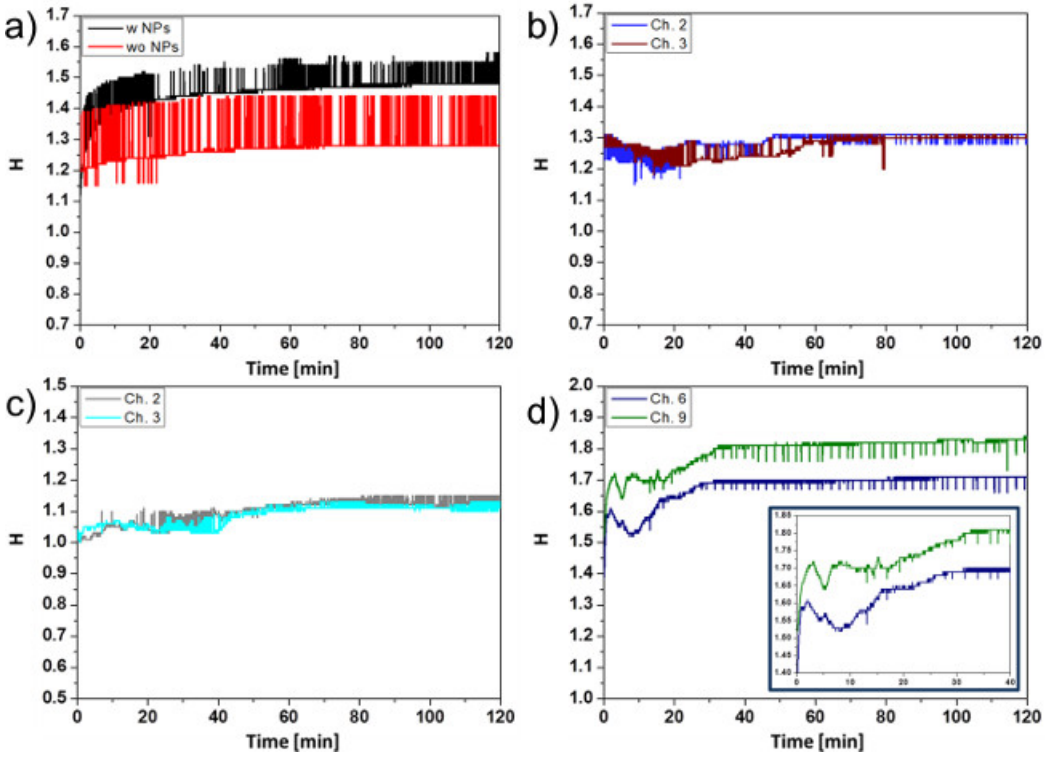

Figure 10: Real-time transistor-transfer function measurements of H441 covered FET devices with and without nanoparticles NexSil20. Presence of nanoparticles (600 µg/ml) does not affect the TTF of the cell-free gates (a). Negative control shows fluctuations in signal amplitude alone with viable cells on the transistor gates (b); while low dose treatment (60 µg/ml) shows slight signal amplitude increase (c). High dose treatment (600 µg/ml) causes visible amplitude value changes in the first 30 min indicating cell apoptosis or necrosis (d). Please click here to view a larger version of this figure.

Supplementary Figure 1: Mask 1: Define contact lines.

Supplementary Figure 2: Mask 2: Define source and drain.

Supplementary Figure 3: Mask 3: Open source and drain contacts and gate area.

Supplementary Figure 4: Mask 4: Lift-off for the source and drain contacts.

Discussion

Silicon FETs have been extensively used in the field of biosensors for different biological applications due to the possibility of minimizing the detection electrodes without affecting their sensitivities. By incorporating the miniature FET devices with impedance spectroscopy, cell adhesion strength down to single cell resolution can be measured in the present study. With the help of simulation results, parameters of a new generation of FET devices have been optimized for measuring cell adhesion[14]. With higher R_{seal} values, generally larger differences between the cell-adhered and the cell-free TTF spectrum can be achieved **(Figure 2)**. In this study, new FET devices with almost flat topography were designed and fabricated **(Figure 5)**. With the flat surface, adherent cells can adhere better and form a tighter junction on top of the transistor **(Figure 6b)**. This will in term enhance the differences of the spectra recorded in FETCIS measurements. Besides, smaller resistances and larger capacitances of the contact lines are beneficial for impedance sensing of cellular adhesion. Therefore all these parameters have been considered and optimized during the fabrication of the FET devices. All steps in the fabrication process of the FET devices are important. Otherwise the fabricated devices may not have the same sensitivities and characteristics as described in the present study.

Significant differences between the cell-adhered and cell-free transistors were observed **(Figure 7)**. Adhesion status of the cells to a protein-coated substrate is important to examine the efficacy and the specificity of drug effects on cancer cells. This is usually studied by microscopic observations. With the presented data it was confirmed that our FETCIS system can be used as an electronic platform for detecting cell adhesion and detachment. In the well-known and established ECIS systems, typically confluent cell cultures are used due to the limitation of recording electrode sizes. However, in many research fields such as immunology and neurosciences, single cell assays would be preferred. Smaller detection electrodes are required for such low density cultures so that individual cell responses can be studied. We presented here, that such low density cultures **(Figure 7)** and even single cell cultures **(Figure 8)** can be applied to our FETCIS system. The sensitivity of FETCIS on single cells is comparable to the sensitivity of ECIS on confluent cultures opening up new possibilities and new assays in Cell-Substrate Impedance Sensing.

Standard methods for studying cell cytotoxicity are normally based on measurements of metabolic activity or membrane integrity of healthy cells using immunostaining techniques and light microscopy. However, results of such methods can be affected by interaction between the tested compounds and the dye. In addition, in most cases end-point live-dead data is obtained. Such methods cannot provide researchers with real-

time data. Our FETCIS method is a label-free, fully electronic approach. No additional dye is required for the measurements. This can minimize the possibility of misleading results due to the interaction of the tested drugs and the dye. Furthermore, the FETCIS system provides real-time monitoring function, which allows studying the effectiveness of the drugs easily **(Figure 9 and Figure 10)**. Please bear in mind that, when the long-term pharmacology study is carrying out, the measurement device must be put inside the incubator for proper environment control.

Our FET devices are robust and therefore can be used for several times after proper cleaning. However, the performances of the devices will still decrease gradually due to the use of H_2SO_4 during cleaning. Therefore, it is important to measure the maximal transconductance value of the devices every time before experiment. When the transconductance value is lowered than 0.2 mS, the FET devices are considered defective and should no longer be used.

In the future, FETCIS could be used with many different cell types. Our novel measurement technique clearly demonstrates single cell resolution, which was the aim in the ECIS community for many years. By far, there is no label-free method, which can be used to measure the direct adhesion strength between cell and substrate in a swift and straightforward manner. We hope that by this publication, we reach a lot of researchers in the field and open a whole-new direction within the biosensor community.

Disclosures

The authors have nothing to disclose.

Acknowledgements

We thank the Federal Ministry of Education and Research (BMBF), Germany for financial support via the project "*Entwicklung eins Zell-Chip Hybrid-Testsystems zur Wirksamkeitsanalyse von Krebsmedikamenten*", 17008X10. We thank A. Offenhäusser, N. Wolters, R. Otto, and D. Lomparski (all at the Forschungszentrum Jülich GmbH, Germany) for the support during the initial start of this project and for the support during development of the TTF amplifier box. The authors thank D. Cassel technical support during chip fabrication and R. Lilischkis (both University of Applied Sciences Kaiserslautern) for SEM imaging.

References

1. Bergveld, P. A critical evaluation of direct electrical protein detection methods. *Biosens. Bioelectron.* **6,** 55–72 (1991).
2. Souteyrand, E. *et al.* Direct Detection of the Hybridization of Synthetic Homo-Oligomer DNA Sequences by Field Effect. *J. Phys. Chem. B.* **101,** 2980–2985 (1997).
3. Schäfer, S. *et al.* Time-dependent observation of individual cellular binding events to field-effect transistors. *Biosens. Bioelectron.* **24,** 1201–1208 (2009).
4. Giaever, I., & Keese, C. R. A morphological biosensor for mammalian cells. *Nature.* **366,** 591–2 (1993).
5. Wegener, J., Keese, C. R., & Giaever, I. Electric cell-substrate impedance sensing (ECIS) as a noninvasive means to monitor the kinetics of cell spreading to artificial surfaces. *Exp. Cell Res.* **259,** 158–66 (2000).
6. Levsky, J. M., & Singer, R. H. Gene expression and the myth of the average cell. *Trends Cell Biol.* **13,** 4–6 (2003).
7. Ingebrandt, S. *et al.* Label-free detection of single nucleotide polymorphisms utilizing the differential transfer function of field-effect transistors. *Biosens. Bioelectron.* **22,** 2834–40 (2007).
8. Koppenhöfer, D., Susloparova, A., Docter, D., Stauber, R. H., & Ingebrandt, S. Monitoring nanoparticle induced cell death in H441 cells using field-effect transistors. *Biosens. Bioelectron.* **40,** 89–95 (2013).
9. Susloparova, A., Koppenhöfer, D., Vu, X. T., Weil, M., & Ingebrandt, S. Impedance spectroscopy with field-effect transistor arrays for the analysis of anti-cancer drug action on individual cells. *Biosens. Bioelectron.* **40,** 50–56 (2013).
10. Regehr, W. G., Pine, J., Cohan, C. S., Mischke, M. D., & Tank, D. W. Sealing cultured invertebrate neurons to embedded dish electrodes facilitates long-term stimulation and recording. *J. Neurosci. Methods.* **30,** 91–106 (1989).
11. Schatzthauer, R. Neuron-silicon junction with voltage-gated ionic currents. *Eur. J. Neurosci.* **10,** 1956–1962 (1998).
12. Ingebrandt, S., Yeung, C. K., Krause, M., & Offenhäusser, A. Neuron-transistor coupling: Interpretation of individual extracellular recorded signals. *Eur. Biophys. J.* **34,** 144–154 (2005).
13. Ingebrandt, S., Yeung, C. K., Krause, M., & Offenhäusser, A. Cardiomyocyte-transistor-hybrids for sensor application. *Biosens. Bioelectron.* **16,** 565–570 (2001).
14. Susloparova, A., Vu, X. T., Koppenhöfer, D., Law, J. K.-Y., & Ingebrandt, S. Investigation of ISFET device parameters to optimize for impedimetric sensing of cellular adhesion. *Phys. status solidi.* **211,** 1395–1403 (2014).
15. Susloparova, A., Koppenhöfer, D., Law, J. K., Vu, X. T., & Ingebrandt, S. Electrical cell-substrate impedance sensing with field effect transistors is able to unravel cellular adhesion and detachment processes on a single cell level.
16. Arndt, S., Seebach, J., Psathaki, K., Galla, H. J., & Wegener, J. Bioelectrical impedance assay to monitor changes in cell shape during apoptosis. *Biosens. Bioelectron.* **19,** 583–594 (2004).
17. Vu, X. T., & Offenhäusser, P. D. A. Silicon nanowire transistor arrays for biomolecular detection. *Faculty of Mathematics, Computer science, and Natural sciences.* **Ph.D,** (2011).
18. Tian, Y-H., Wang, C-Q., Zhou, Y. N. Bonding mechanism of ultrasonic wedge bonding of copper wire on Au/Ni/Cu substrate. *Trans. Nonferrous Met. Soc. China (English Ed).* **18,** 132–137 (2008).

